Proceedings of ASME Turbo Expo 2004
Power for Land, Sea, and Air
June 14-17, 2004, Vienna, Austria

GT2004-53361

FLOWFIELD MEASUREMENTS IN A RIBBED CHANNEL RELEVANT TO INTERNAL TURBINE BLADE COOLING

A. Graham, E. Sewall and K. A. Thole
Mechanical Engineering Department
Virginia Polytechnic Institute and State University
Blacksburg, VA 24061

ABSTRACT

The internal cooling of turbine blades is an important part of overall blade cooling that is necessary to survive current turbine inlet temperatures. This internal cooling is often performed by means of rib-turbulated passages designed to provide maximum heat transfer coefficients. One determining factor in the cooling effectiveness is the flow pattern created by the ribbed channel. This paper presents a comparison of the effect of two different channel blockage ratios on the fully developed flow pattern in a stationary ribbed channel.

For the experimental investigation, a scaled-up ribbed passage was tested using a closed-loop channel facility. The facility included a passage consisting of a developing region, a fully developed region, a 180° bend, and a second developing region following the bend. Friction factors were determined through the use of pressure taps throughout the channel, and flow fields were measured using a two-component laser Doppler velocimeter. A majority of the testing performed was done under conditions of in-line (i.e. non-staggered) ribs with ratios of rib height to channel hydraulic diameter of 0.10 and 0.17. All LDV measurements were performed at a Reynolds number of 20,000.

Results indicate that both blockage ratios create significant recirculation regions immediately before and immediately following the rib. While the smaller rib results indicate a reattachment downstream of the rib, the larger rib results indicate that the flow is separated along the entire streamwise distance between the ribs. The smaller blockage ratio also indicated a small recirculation region directly on top of the rib, whereas the larger blockage ratio showed no such region. Additionally, the increased friction factor created by the larger ribs can be attributed to the larger recirculation regions between ribs.

INTRODUCTION

The internal cooling of blades and vanes has become an important issue for the gas turbine industry as decreasing component temperatures increase the life of the airfoils. To decrease component temperatures in the turbine section of a gas turbine engine, high pressure air from the compressor that is much cooler than the hot combustion gases passing over the turbine airfoils is passed through turbine airfoils prior to being expelled through film cooling holes placed in the airfoil surfaces. As the flow passes through the airfoils, the objective is to convectively cool the inner airfoil surfaces and, as such, high convective heat transfer coefficients are desired. These internal channels are often ribbed surfaces whereby the objective of the rib is to promote turbulent flow and subsequently enhance the heat transfer between the channel walls and coolant. Though these channels are built in a wide range of cross-sectional shapes and aspect ratios as a result of the airfoil geometry, many sections of these channels can be approximated by square or trapezoidal cross-sectional areas.

While there have been a large number of studies completed in this research area, as will be described in the next section, there have been relatively few studies reporting measured turbulence levels for a ribbed channel flow relevant to turbine airfoils. The primary objectives of the work presented in our paper are the following: i) determine the length required for a ribbed channel flow to become fully developed, ii) address flowfield differences in two different rib configurations with different rib heights, and iii) compare the turbulence augmentation of a ribbed channel to that of a smooth channel wall. Moreover, as there is a desire to further computational capabilities in predicting internal flows such that computational fluid dynamics (CFD) becomes a useful design tool, there is a need for benchmarking data. The remainder of this paper describes past studies that are relevant to our work, the experimental set-up and benchmarking and, finally, the measured flow fields.

RELEVANT PAST STUDIES

One aspect of this work that was considered was where to define the length of the hydrodynamic entry region within a ribbed channel. A number of different methods have been

reported in the literature, including the following: i) location where static pressure measurements indicate a constant friction factor, ii) location where heat transfer measurements indicate a constant coefficient, and iii) location where the mean velocity profiles in the channel have a similar shape. As such, there is a large variation in reported entry region lengths for ribbed channels with ribs positioned orthogonal to the flow ($\alpha = 90°$). As an example, Liou et al. [1] stated that the flow was fully developed after the third rib based on their pressure coefficient measurements in a high aspect ratio channel with a rib height-to-channel height ratio (e/H) of 0.13 and a rib pitch-to-height ratio (P/e) of 10. Based on their surface heat transfer measurements in a square channel, Han et al. [2] showed that a developing length of six ribs was required for $e/D_h = 0.047$, which is half the rib height of the previous study, and P/e = 10. Based on these two studies one could postulate that an increase in development length was proportional to the e/D_h ratio. An example of the third criteria mentioned above is given by Rau et al. [3], who determined that flow was developed after four ribs based on mean velocity measurements in the symmetry plane attaining periodic conditions.

Others who have identified the streamwise length required to become fully developed include the mass transfer studies by Sparrow et al. [4] between parallel plates with round disturbance rods with diameters of e/H = 0.082 and 0.164 (where H is the channel height) and spacing of P/e = 10. They observed a virtual absence of an entrance region based on a periodic distribution of the Sherwood number along the roughened wall. As another example, consider Han [5] who presented studies for a square channel with rib heights of $e/D_h = 0.063$ and rib spacing of P/e = 10. In this study he defined the beginning of the thermally fully developed region as the point at which wall and fluid temperatures increased linearly as a function of streamwise position. As such, they stated that between 13 to 15 ribs were required to achieve thermally developed flow for this rib configuration. Typical accepted values, however, throughout the literature are between three and seven ribs for a developing flow region in a channel with two ribbed walls.

Another aspect of the work presented in this paper is the effect that the rib height has on the resulting flow fields. The rib heights along with the number of ribbed walls determine the amount of channel blockage the flow encounters. In a study where the rib height was varied from $e/D_h = 0.021$ to 0.063, both the average friction factor and Stanton number were shown to increase with rib height in a square channel with rib spacing of P/e = 10 (Han [5]). Taslim et al. [6] indicated similar findings for his staggered rib configuration with three different heights ranging from $e/D_h = 0.133$ to 0.250. When the rib height ratio (e/D_h) was increased and the pitch ratio (P/e) was kept constant, channel heat transfer was found to increase. However, an increase in rib height (e/D_h increasing from 0.133) while not keeping the rib spacing constant (P/e decreasing from 10 to 5) resulted in a decreased heat transfer enhancement with the increase in friction factor.

Internal channel studies that focus on frictional losses and surface heat transfer alone can compare the effects of geometry variations but do not provide an understanding of the flow mechanisms. In particular, it is important to consider the mean and turbulent flow characteristics inside of a ribbed channel since it is these characteristics that govern the overall heat transfer in a cooling channel. There are relatively few studies that have resolved the flow fields of ribbed channels, which include the work of Liou et al. [7], Rau et al. [3], Chanteloup et al. [8], and Casarsa et al. [9]. Liou et al. found a maximum turbulence level (when defined similar to Tu in this paper) of approximately 37% in the shear layer behind the rib, and the work by Rau et al. showed that the maximum turbulence levels occurred in the same location with levels as high as 30% (when defined similar to the current study). Chanteloup et al. studied a channel with ribs of $\alpha = 45°$, but did not report any specific turbulence quantities. Casarsa et al. described streamwise fluctuations as high as 80% in the shear layer downstream of the rib for rib heights of $e/D_h = 0.30$. In the center channel, turbulence levels calculated from rms quantities reported by Rau et al. came out to 13%, and turbulence calculated from data reported by Liou et al. was 20% in the center. Moreover, their results showed the existence of three recirculating regions in the streamwise direction for these large rib heights that included the following: one just downstream of the rib that encompassed the largest region, one just upstream of the rib, and one on top of the rib.

To the authors' knowledge, a comparison of the enhancement of turbulence at the two rib heights and a smooth channel presented in this paper has not been made. This study reports on the evolution of the turbulence profiles between two ribs for two different rib heights and their comparison to a smooth channel flow.

EXPERIMENTAL FACILITY TECHNIQUES

The data included in this paper, flow field and pressure drop measurements, were made in a ribbed channel facility with two different rib heights. Figure 1a shows an overall schematic of the facility, which was a closed-loop design. Air was supplied to the channel by means of a 2 hp fan. Downstream of the fan, the air passed through a large diffuser, a heat exchanger, and a nozzle having an area ratio of 10:1. The nozzle was designed through computational fluid dynamics (CFD) simulations to give a uniform inlet profile at the entrance to the channel. The ribbed channel of square cross-section (aspect ratio of 1:1) consisted of a straight section, followed by a 180° sharp turn, followed by another straight portion. Upon exiting the return leg of the test section, the air passed through a venturi flowmeter before returning to the fan. The venturi flowmeter was calibrated against a laminar flow element whereby the laminar flow element was calibrated by the manufacturer. The venturi was used rather than the laminar flow element because it incurred a lower pressure drop to the system. Coarse adjustments to the flowrate were made using a large gate valve immediately upstream of the fan, while fine adjustments were made using a motor controller connected to the fan. All of the flow field measurements were performed at a Reynolds number of 20,000, which was set based on the bulk velocity as calculated from the venturi flowmeter. Air temperatures and absolute pressures were also taken into account in this calculation with both being measured just before the inlet to the test section.

The test section, which was designed to insure good measurement resolution while matching an ongoing CFD simulation to be presented at a later time, included a square channel made of Lexan. Lexan provided a surface that was optically acceptable for the laser Doppler velocimeter (LDV)

measurements. The inner channel width and height were 14.9 cm with a wall thickness of 0.95 cm. The channel was approximately 3.53 m in length upstream of the 180° sharp bend that maintained the same channel dimensions (Figure 1b). The downstream leg of the ribbed channel extended another 1.47 m.

A fully developed section of the channel is pictured in Figure 1c. The corresponding dimensions for the two cases studied are given in Table 1. Attached to the bottom and top walls of the channel were ribs machined from Delrin, which is a low friction, inflexible polymer. The ribs for the baseline cases were square in cross-section with a rib height of 1.49 cm ($e/D_h = 0.1$). To increase the rib height, Lexan covers were placed on top of the ribs to increase the height to $e/D_h = 0.17$, which in turn decreased the pitch to $P/e = 6$. The location of the first rib was placed at 6.7 cm (0.45 rib pitches) downstream of the contraction exit, which is 4.5 rib heights for the baseline case and 2.7 rib heights for the larger ribs.

Prior to making the LDV measurements, pressure drop measurements were completed for a range of conditions to allow friction factors to be compared with those found in the literature for nearly the same geometry. To determine the increased frictional losses resulting from the ribs, pressure taps were installed along the entire channel length of the smooth side wall that were spaced 14.9 cm apart and located directly between the ribs. These static pressure taps were connected to

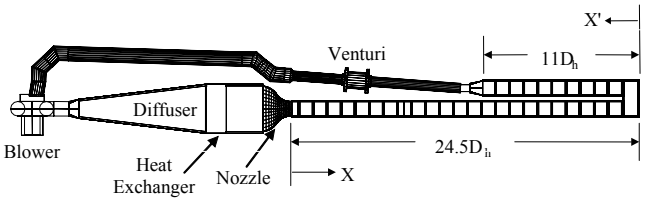

Figure 1a. Schematic of ribbed channel facility.

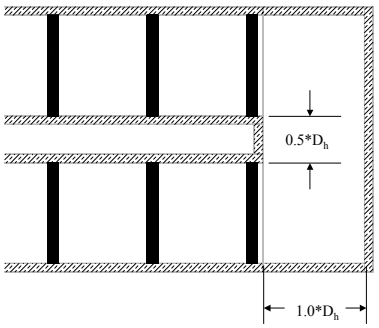

Figure 1b. Illustration of 180º bend in test section.

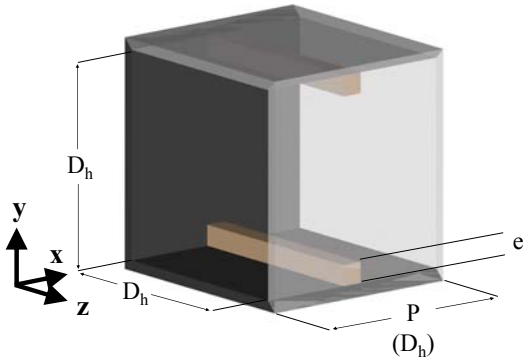

Figure 1c. Illustration of the coordinate system.

Table 1. Rib Geometrical Parameters

	Small	Large
Rib angle (α)	90°	90°
P/D	1	1
P/e	10	6
e/D	0.10	0.17
Channel Aspect Ratio	1	1
Rib Configuration	Symmetric	Symmetric
Ribs in Upstream Leg	24	24
Ribs in 180° Bend	0	0
Ribs in Downstream Leg	10	10
Re	20,000	20,000

a scanivalve that was in turn connected to a differential pressure transducer. The pressure transducer range was 0.25 in. H_2O. Friction factors were calculated based on the following equation relating differential pressure and friction factor:

$$f = \frac{\Delta p \ D_h}{2 \ \Delta x \ \rho u_b^2} \qquad [1]$$

where Δp is the static pressure difference measured over the given streamwise distance Δx. Both average friction factors as well as local friction factors were calculated. The average friction factors included all of the ribs extending from the fourth rib to the 23rd rib. The normalizing relation for the friction factors was the Blasius correlation:

$$f_o = 0.046 \ Re^{-0.2} \qquad [2]$$

Flowfield measurements for this study included the mean and the corresponding root-mean-square (rms) velocities. A two-component back-scatter fiber optic LDV system was used in this study that consisted of a 5 Watt laser and a TSI model 9201 Colorburst beam separator. Velocity data was processed using TSI model IFA 755 Digital Burst Correlator controlled using TSI's FIND software. The LDV was positioned on the side of the test channel to capture the streamwise (u) and vertical (v) components of the velocity. To capture the smallest control volume, a 450 mm focusing lens was used in conjunction with a beam expander. The probe volume length and diameter were 0.32 mm and 44 microns, respectively. The LDV probe was tilted at 10°, to allow for measurements very near the surface. For the LDV measurements, each mean and rms velocity was averaged between 10,000 and 20,000 points, which took nominally 20 seconds to acquire. All measurements were corrected for bias errors using the well-accepted time weighted average correction scheme. The flow was seeded using olive oil having a particle diameter of nominally 1 micron.

Overall uncertainties were calculated for the friction factors and flow field measurements according to the partial derivative method described in Moffat [10]. The total uncertainty of all measurements was calculated as the root of the sum of the squares of the precision uncertainty and the bias uncertainty. The precision uncertainty was based on a 95% confidence interval. Uncertainties were calculated based on a 95% confidence interval. The estimate of bias uncertainties for the mean velocities was 1%. The precision uncertainty for the streamwise rms velocities was 2.6%. For the friction factors, the uncertainty was calculated to be 6%.

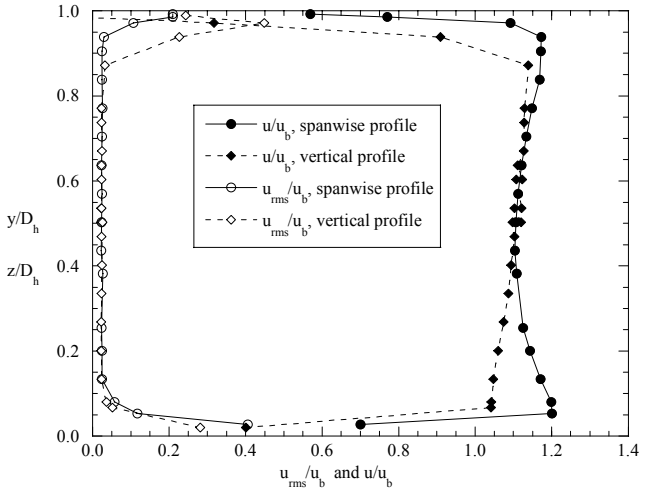

Figure 2. Inlet velocity profiles at 0.21D_h downstream of the contraction exit.

BENCHMARK STUDIES FOR THE RIBBED CHANNEL

A number of studies were completed prior to acquiring the flow field data to benchmark the ribbed channel. These studies included measurements of the inlet velocity profiles (exit of the contraction) and velocity profiles in the fully developed portion of the channel to verify symmetry and measurement repeatability. Friction factor studies were completed to compare with data found in the literature. Figure 2 shows the LDV measurements of vertical and spanwise velocity profiles taken 0.21D_h (31 mm) downstream of the contraction into the test section. The vertical profile was taken at mid-channel span and the spanwise profile was taken at mid-channel height. It can be seen from Figure 2 that the inlet profiles were relatively uniform with the wall effects being 0.1 of the channel. The incoming turbulence level at the channel mid-span was 2%.

To determine whether the flow was symmetric within the fully developed portion of the channel full profiles were taken across the channel with the smaller rib height of $e/D_h = 0.1$. Symmetric conditions reduce the required measurements to document the flow field by a factor of two. Both the mean and root-mean-square (rms) of the velocity fluctuations were measured horizontally between the two smooth walls halfway between the two ribbed walls (Figure 3a) and vertically between the two ribbed walls halfway between the two smooth walls (Figure 3b). Both profiles were taken above the 13th rib downstream of the inlet ($X = 12.5D_h$). Figures 3a and 3b show the top half and bottom half profiles superimposed on one another. There is a slight difference in the mean velocities in Figure 3a, but for the most part all of the profiles indicate symmetric conditions. These profiles show that the channel flow is symmetric. It is also interesting to note the increase in turbulence level caused just above the rib.

Comparisons were also made to determine the flow periodicity for the smaller rib height of $e/D_h = 0.1$ as shown in Figure 4. These profiles were acquired for the mid-region upstream and downstream of the 12th rib. If the flow is periodic, we would expect the profiles to lie on top of one another and, as shown in Figure 4, these profiles do. The strong agreement between these profiles is an indication that the flow is hydrodynamically fully developed in this region. Figure 4 also shows that the peak rms level of the streamwise

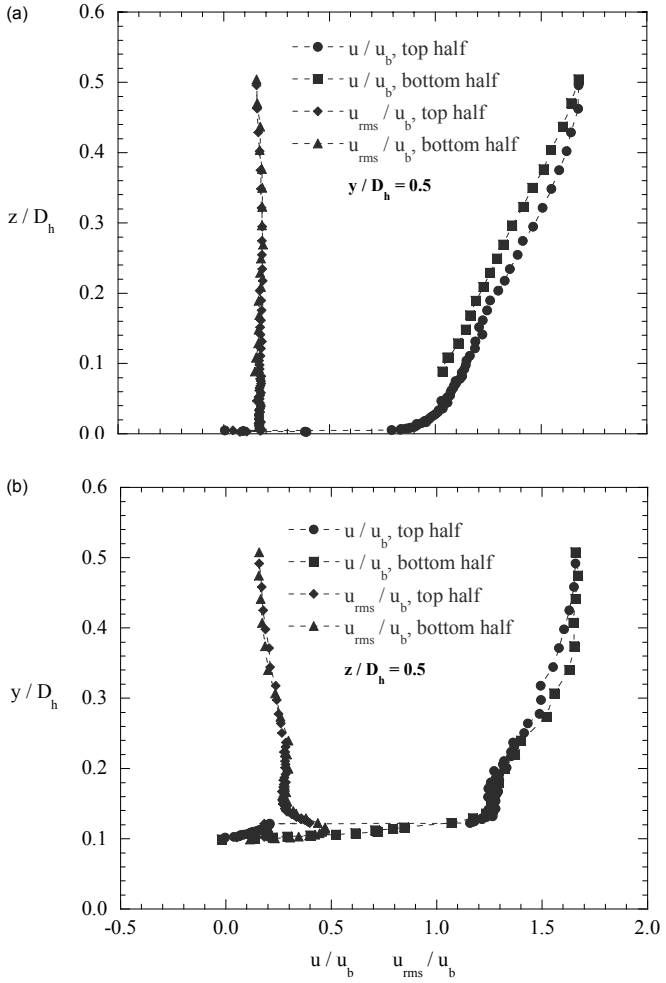

Figure 3. Mean and rms velocity profiles showing flow symmetry in the (a) z-direction and (b) y-direction at the 13th rib (X = 12.5Dh) at Re = 20,000.

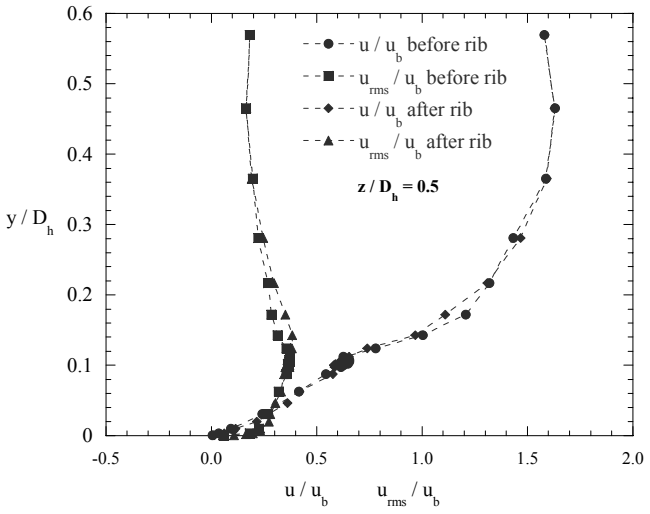

Figure 4. Velocity profiles between ribs in the fully developed region illustrating periodicity for the 12th rib for $e/D_h = 0.10$ at Re = 20,000.

velocity fluctuations mid-way between the ribs is aligned with y/Dh = 0.1, which is the height of the rib.

The final benchmark that was completed for the channel prior to making measurements was to compare measured friction factors with those found in the literature for ribbed channels. Friction factors were determined for various rib geometries, including in-line and staggered rib configurations with blockage ratios of e/D_h = 0.10, 0.133, and 0.17. All of these friction factors were measured at a flow Reynolds number of 30,000 to match data available from other researchers. Comparisons were made by using the measured pressure drop from the fourth to the 23rd rib. As will be discussed later, the flow did not become fully developed until the tenth rib in some cases based on the flow field measurements but the pressure drop measurements indicated no change in the friction factors beyond the fourth rib.

Figure 5 shows the comparison of friction factor data for several geometries and researchers as well as our measurements. As can be seen, the data from the current studies falls well within the range of that by other researchers. The friction factor data indicates, as others have shown, there is a strong dependence on the rib height (e/D_h ratio), but only a small effect of rib pitch and, although it is not shown, Reynolds number. It is also clear as to the substantial increase in pressure losses that occur for a ribbed channel relative to a smooth channel. For the largest rib height, the frictional losses are as much as 19 times higher than that for a smooth wall. As such, it is instructive to better understand why there is such a large effect of rib height on the friction factors.

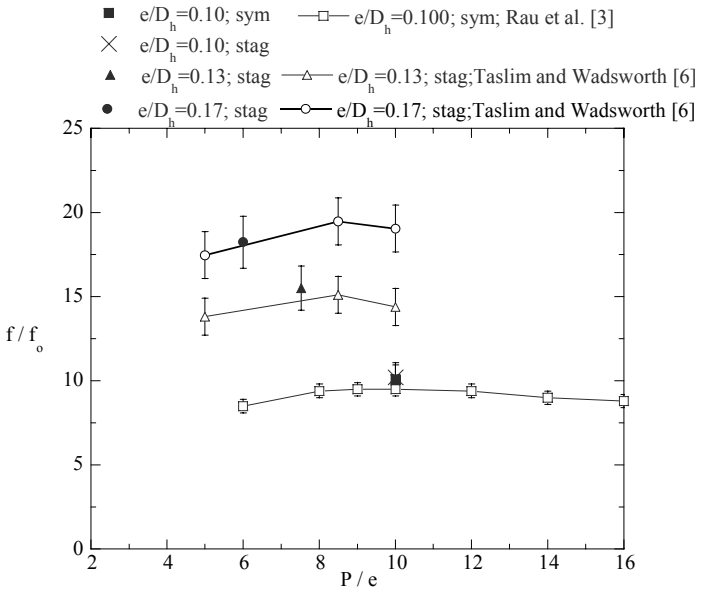

Figure 5. Friction factor data as compared with other researchers at Re = 30,000.

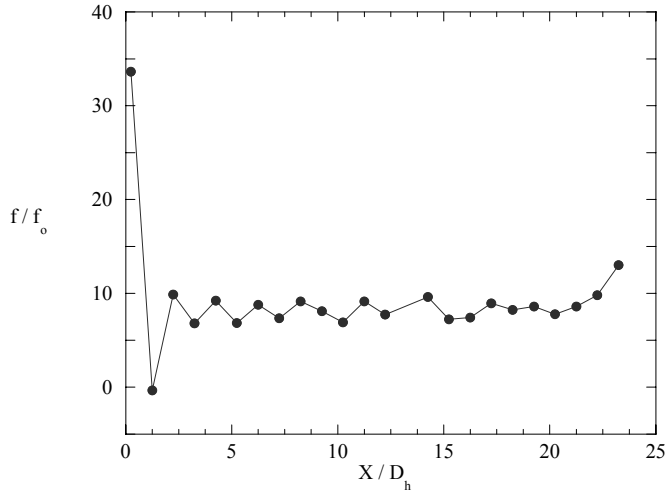

Figure 6. Friction factors along the length of the ribbed channel for e/D_h = 0.10 at Re = 20,000.

ENTRANCE REGION EFFECTS

As was discussed in the previous studies, there are a variety of methods used in the literature to define the entry region of a ribbed channel. In the work presented in this paper, comparisons of flow field measurements to that of pressure drop measurements along the smooth wall were made in defining the start of the fully developed region.

Using the pressure taps installed along the length of the smooth channel wall, it was possible to determine the development of the friction factor as flow progressed in the streamwise direction. Figure 6 shows the development of the local friction factor for a rib blockage ratio of e/D_h = 0.10 at

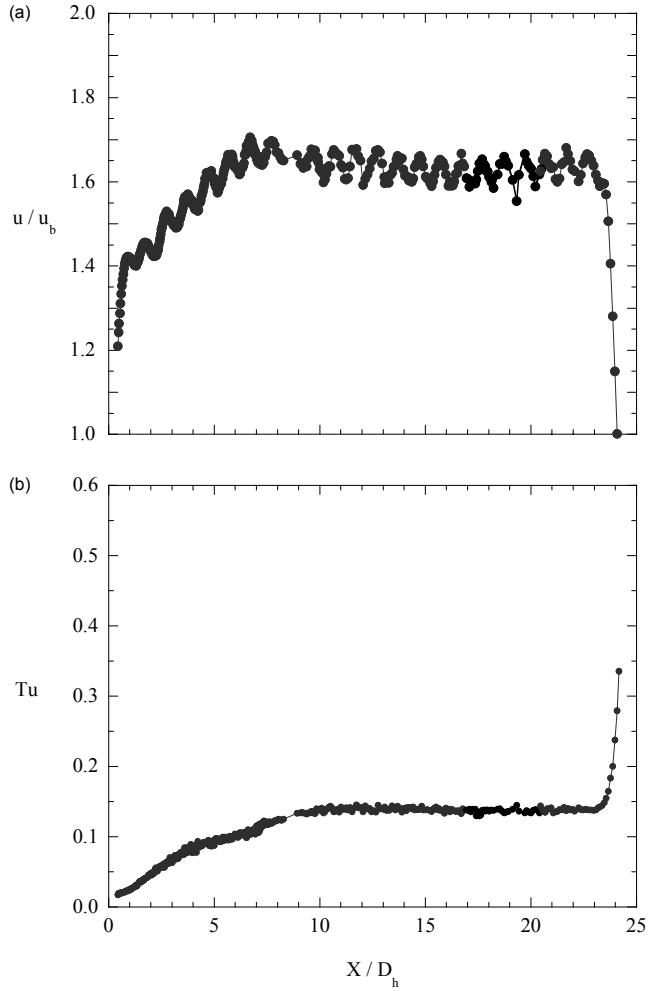

Figure 7. Center channel measurements of the (a) mean streamwise velocity and (b) Tu along the ribbed channel for e/D=0.10 at Re = 20,000.

Re = 20,000. It is clear from this data that one could interpret the entry region to be approximately 3-5 ribs, which is a value that agrees with results by previous researchers [1-3].

Flow field measurements, however, indicate a longer development length than that indicated by the friction factor. Figures 7a and 7b show the bulk-normalized streamwise velocity and rms velocity as a function of the streamwise location along the channel. These measurements were taken at mid-channel span and mid-channel height. Although the velocity continually oscillates due to the periodic ribs, it can be seen that the flow does not become fully developed until the 10th rib. Additionally, Figure 7b shows the development of the normalized rms of the streamwise velocities as a function of the streamwise location. The data shown in Figure 7b also illustrates that the flow became fully developed by the tenth rib.

Comparisons of Figures 6 and 7 illustrate that while the pressure measurements indicate the flow is fully developed by the fourth rib the flow field measurements indicate the flow is not fully developed until the tenth rib. As such, it is important to allow a long enough development length for ribbed channel studies to insure fully developed conditions exist. Assuming the flow is fully developed based on the static pressure measurements taken along the smooth wall of a ribbed channel leads to an underestimate in the development length.

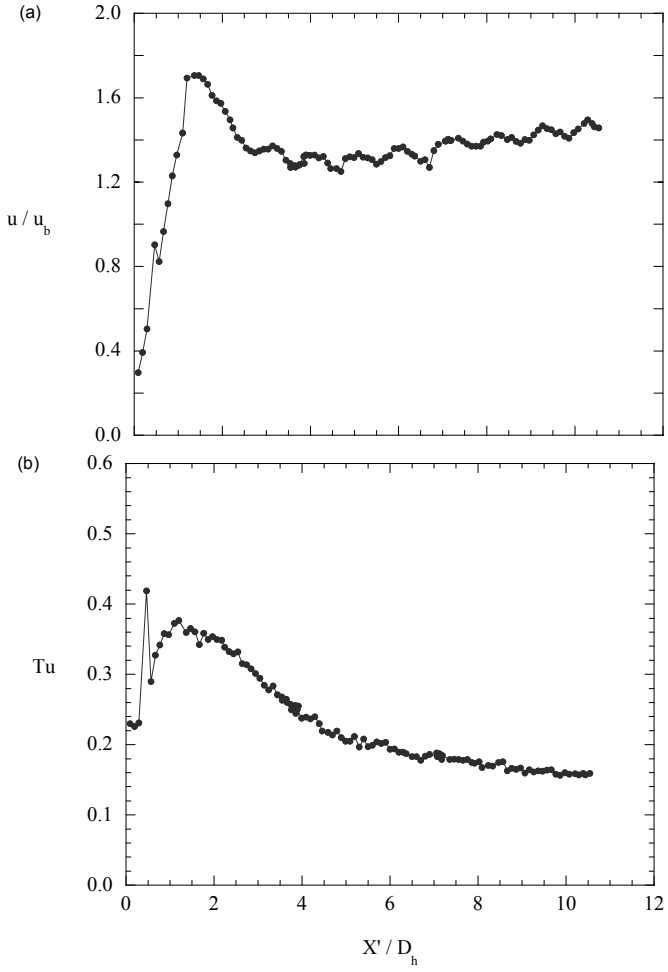

Figure 8. Measurements downstream of the return leg of the (a) mean streamwise velocity and (b) Tu along the ribbed channel for e/D=0.10 at Re = 20,000.

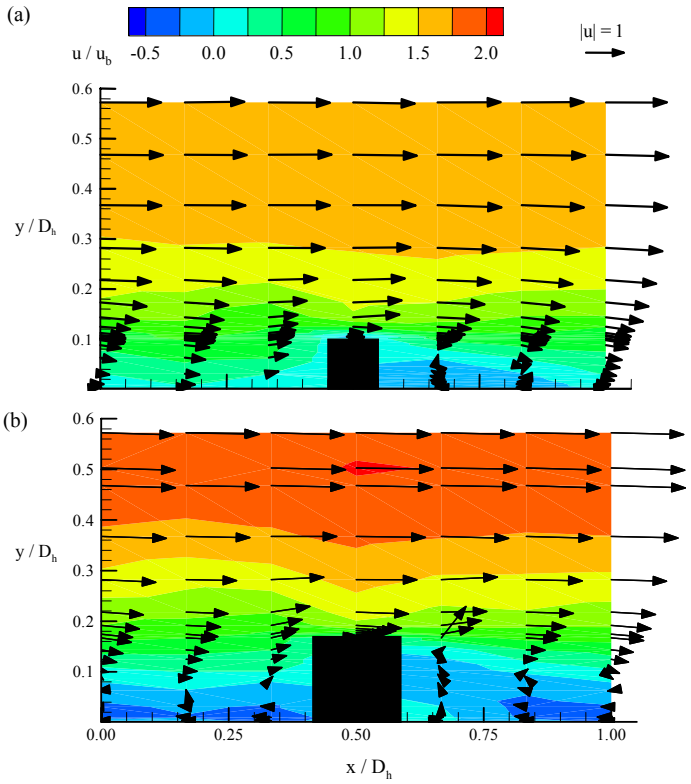

Figure 9. Velocity contours superimposed on the vector plots for (a) $e/D_h = 0.10$ and (b) $e/D_h = 0.17$ measured at the spanwise center of the channel ($z/D_h = 0.5$) starting at 12th rib at Re = 20,000.

Another important region of most ribbed channels is that downstream of the bend. Figures 8a and 8b show the development of the flow as it exits the 180° bend. Again, these measurements were taken at mid-channel span and mid-channel height. Lower overall values were measured at this location because of the skewing of the velocity profile caused by the bend region. It is evident that the length required to reach fully developed flow exiting the bend region is much longer than the 10 ribs required for the entrance region. These results indicate that with a uniform inlet profile the development region is shorter as compared to a situation with a skewed profile.

FLOWFIELDS FOR DIFFERENT RIB HEIGHTS

Flowfield measurements were acquired along the 12th rib for the two different in-line rib configurations with an e/D_h = 0.10 and 0.17. The streamwise velocity contours and mean velocity vectors for both rib sizes are shown in Figures 9a-9b while the turbulence levels are shown in Figures 10a-10b. The mean flow field data (Figures 11a-11b) clearly show that near mid-channel, the peak velocity is 1.6 times that of the bulk velocity for the e/D_h = 0.10 and 2.0 times that of the bulk velocity for e/D_h = 0.17. More importantly, there is a significantly larger recirculation region upstream of the rib for the larger rib as compared with the smaller rib. The recirculation regions in a fully developed channel have been described by Rau et al. [3] and observed here. For the smaller rib case, the flow reattaches at a location approximately halfway between ribs. The flow then separates again just

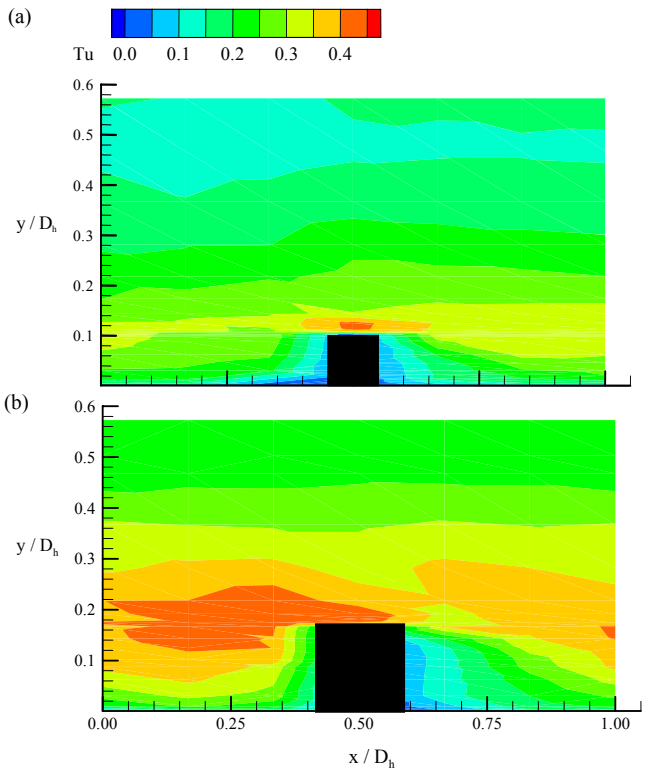

Figure 10. Turbulence contours for (a) $e/D_h = 0.10$ and (b) $e/D_h = 0.17$ measured at the spanwise center of the channel ($z/D_h = 0.5$) starting at 12th rib at Re = 20,000.

upstream of the rib, creating another small recirculation region. For the larger rib case, however, the flow does not reattach between ribs, but instead recirculating flow is present along the entire distance between ribs.

Another important characteristic in the two measured flow patterns is the existence of a small recirculation region directly on top of the smaller rib that is not observed in the larger rib. This is seen by the negative streamwise velocity on top of the rib in Figure 11b. This recirculation zone has been observed on top of large ribs ($e/D_h = 0.3$) by Casarsa et al. [9]. Casarsa et al. showed the recirculation region to occur on the top of the rib on the windward portion with the reattachment occurring upstream of the center of the rib top. The absence of this separation region in our measurements is most likely because of a lack of measurement resolution with only one profile acquired at the center of the rib top. The mean velocity profiles for the large rib case indicate that there is a core flow with a large separated flow region between the ribs. The top of the large ribs effectively act as a virtual wall rather than a true wall of the channel. For the small rib case, however, the flow below the top of the rib is able to flow up and over the rib separating at the top of the rib over a larger portion of the rib top.

Contour plots of the rms velocities for the small and large ribs (Figures 10a-10b) compare the effect that the rib size has on the turbulence production. These contours illustrate the fact that the turbulence located in the core of the flow is significantly higher for the e/Dh = 0.17 case than for the 0.1 case. Around the rib itself, low fluctations were measured, but it is important to remember that the local mean velocity is very low at these locations (recall that one normalizing velocity was

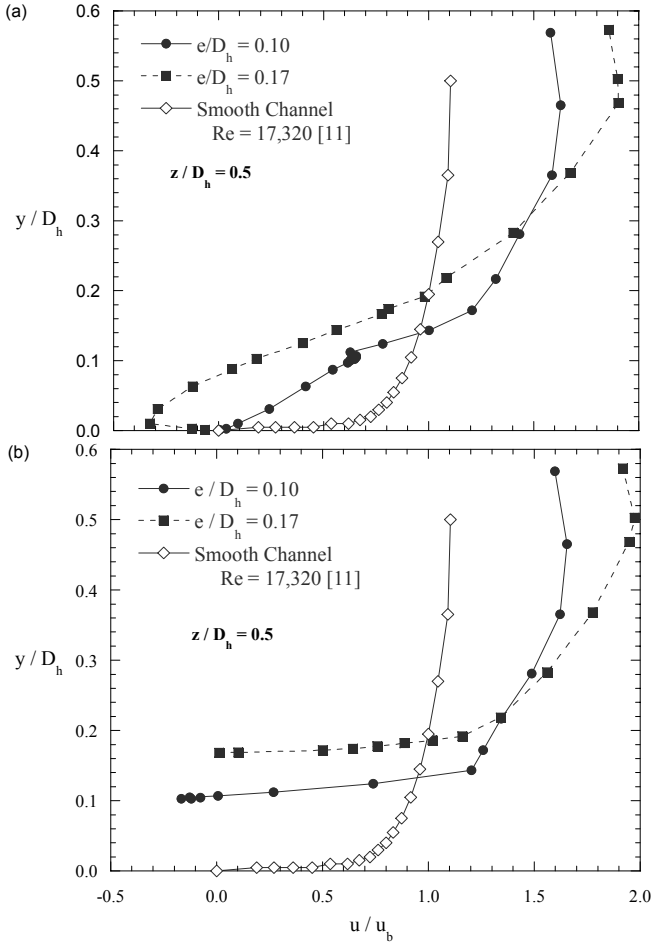

Figure 11. Streamwise velocity measurements (a) between two ribs and (b) on top of a rib at the 12th rib as compared to the smooth channel data of Harder and Tiederman [11].

used for these rms levels, which was that of the bulk velocity). One of the most important areas to contrast is the turbulence levels on top of the rib. While the high turbulence extends throughout the entire rib pitch for the large rib height, it is much more localized to a region on top of the rib for the small rib height.

Despite the fact that these high turbulence levels exist for the large ribs, which generally means a higher heat transfer level, the results of Taslim et al. [6] showed that the heat transfer is relatively low for ribs this large when the rib pitch ratio (P/e) is not held constant to account for rib height. The reason for this is because there is slow fluid re-circulating between the ribs thereby not convecting the heat from the channel walls. This causes a decrease in heat transfer enhancement and is further characterized by an increased pressure drop where the blockage of the large ribs causes a pressure drag loss resulting in high friction factors.

COMPARISON TO A SMOOTH CHANNEL

A quantitative comparison of the turbulence enhancement of the rib turbulators over a smooth channel is an important part of understanding the effect of ribs on channel flows. Knowledge of the changes imposed on the flow field by the ribs aids in understanding both the positive heat transfer

augmentations as well as the negative frictional losses, both of which are highly important when considering turbulated flows.

In this study, velocity profiles were measured from the wall to the channel mid-height for two different rib heights. A comparison of the mean streamwise velocity and streamwise fluctuations is made to that of smooth channel data taken by Harder and Tiederman [11]. Note that the data acquired for the smooth wall was at a Re = 17,320. All velocities and turbulence quantities are non-dimensionalized by the channel bulk velocity.

The mean velocities are compared in Figure 11 mid-way between the ribs and on top of the ribs. One defining aspect of the velocity profiles due to rib size is the amount of mass flow directed towards the center of the channel, as is seen from the larger velocities in the center channel as a result of the rib blockage effects. This results in slower mean velocities near the wall, where heat transfer takes place. Another defining feature of the rib velocity profiles is the negative velocity seen near the wall in the case with the larger ribs. This is a result of the area between the ribs being within the recirculation region.

The streamwise velocity fluctuations, u_{rms}, are plotted in Figure 12 and show a dramatic difference between the three cases. The larger rib height significantly increases the turbulence throughout the channel. The addition of ribs, over a

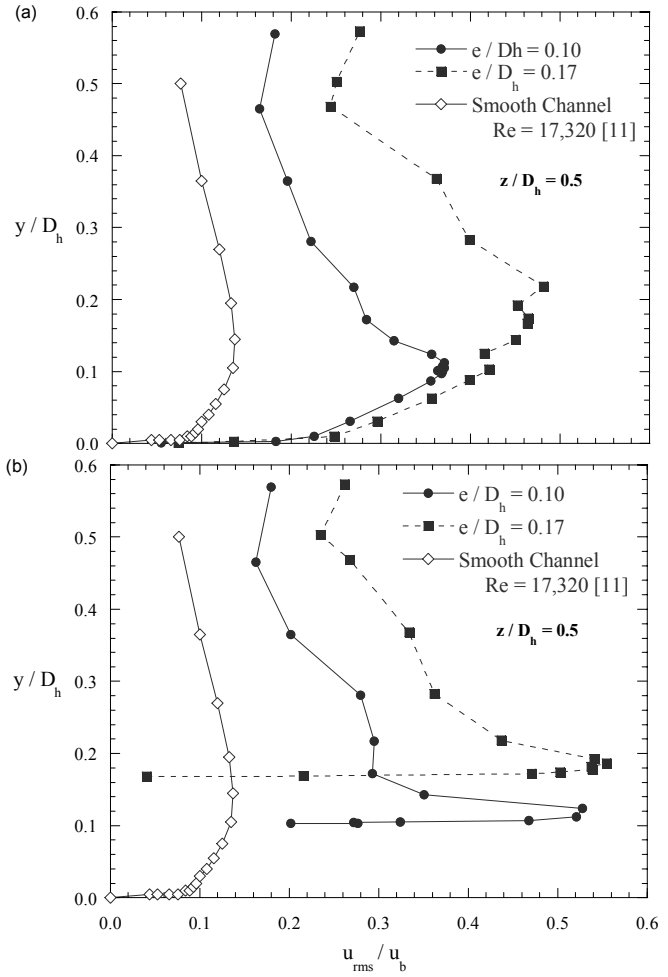

Figure 12. Streamwise rms fluctuations (a) between ribs and (b) on top of a rib at the 12th rib as compared to the smooth channel [11].

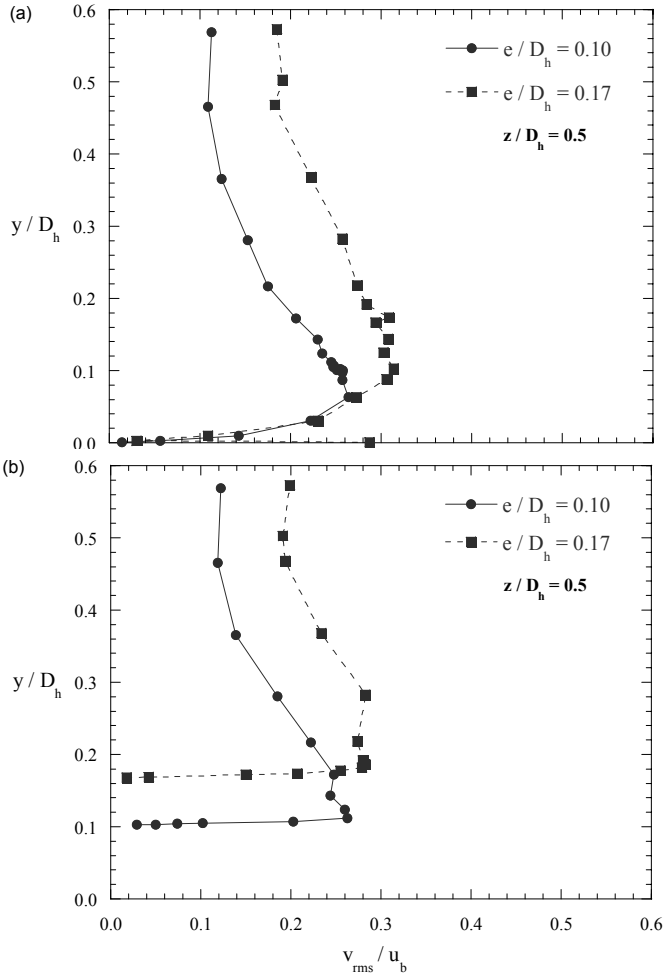

Figure 13. Vertical rms fluctuations (a) between ribs and (b) on top of a rib at the 12th rib at Re = 20,000.

smooth channel flow, increases the streamwise fluctuations from a maximum of 14% to a maximum of greater than 35%, which is an increase by a factor of 2.5. This turbulence is enhanced even more with the larger ribs to values nearly up to 50%. Turbulence is lowest in the center of the channel, having values of about 8%, 17%, and 25% for the smooth channel, small ribs case, and large ribs case, respectively. One interesting aspect to note is the turbulence enhancement near the wall. The small ribs greatly enhance this over a smooth channel, but almost no enhancement is seen when the large ribs are compared with the small ribs. Given that studies [6] have indicated a reduction in heat transfer for the larger rib case, this reduction is occurring as a result of the mean flowfield conditions and not because the turbulence level is reduced in the near wall region. The streamwise turbulence profiles above the ribs (Figure 12b) show the high-turbulence region immediately above the ribs. This is a result of flow separating and accelerating past the rib. This has been observed in many previous studies, e.g. Rau et al. [3].

The vertical turbulence fluctuations are plotted in Figure 13. Similar results are seen in this figure, where these fluctuations are enhanced uniformly throughout most of the channel with the larger rib size providing higher fluctuations. At the center channel the increased rib size is shown to double

the rms levels. As would be expected, the wall dampens the vertical fluctuations such that similar profiles occur near the wall. The profiles above the ribs (Figure 12b) show very little difference for the two rib sizes with the exception of a vertical shift. The highest vertical fluctuations are seen above the ribs.

CONCLUSIONS

An experimental study on a ribbed channel, representative of internal cooling in a turbine airfoil, was conducted to determine why there are such large frictional losses with minimal heat transfer benefits as the rib height is increased. The focus of the work was first to benchmark the facility by comparing with measured pressure drop data from the literature. Good agreement was found for a number of cases.

It was identified that two different answers could be derived, dependent on the method used, with regards to the length of the developing region for a ribbed channel. In comparing the flow field measurements with static pressure measurements along the smooth side wall of the ribbed channel, the flow field measurements indicate the need for ten ribs while the static pressure measurements indicate only a need for four ribs. The flow field, particularly the turbulent fluctuations, requires some streamwise distance to allow the fluctuations to convect to the channel center.

Flow field measurements were compared for in-line ribs placed on two of the four channel walls for a square channel with rib height-to-hydraulic diameter ratios of 0.10 and 0.17. These measurements indicated a large recirculating region between the ribs for the larger rib height. While the pressure losses were found to be very high for the large ribs, the literature indicates a decrease in heat transfer as the rib height is increased and the ratio of rib pitch-to-hydraulic diameter is decreased. The increase in turbulence levels for the larger rib would suggest higher heat transfer, but the literature indicates a reduction in the heat transfer for these large ribs. This decrease in the heat transfer can be attributed to the recirculating flow between the ribs as compared with a reattached flow pattern that occurs for smaller rib heights. The turbulence produced by the ribs relative to that of a smooth channel indicates centerline values that are as much as a factor of two higher for the smaller ribs and three higher for the larger ribs.

ACKNOWLEDGMENTS

This publication was prepared with the support of the US Department of Energy, Office of Fossil Energy, National Energy Technology Laboratory. However, any opinions, findings, conclusions, or recommendations expressed herein are those of the authors and do not necessarily reflect the views of the DOE.

NOMENCLATURE

D_h	=	channel hydraulic diameter, characteristic length
e	=	rib height
f	=	local friction factor
H	=	channel height
Δp	=	local pressure drop across one periodic rib
P	=	rib pitch
Re	=	Reynolds number $D_h \cdot u_b / \nu$
rms	=	root mean square
Tu	=	turbulence level given as: $Tu = \sqrt{0.5(u_{rms}^2 + v_{rms}^2)} / u_b$
u	=	streamwise local velocity
u_b	=	mass averaged velocity, characteristic velocity
v	=	vertical local velocity
x	=	local streamwise position
X	=	global streamwise position relative to exit
X'	=	global streamwise position downstream of bend
Δx	=	change in position across one periodic rib
y	=	local vertical position
z	=	local spanwise position
α	=	rib angle of attack
ρ	=	fluid density
ν	=	kinematic viscosity of the fluid

REFERENCES

[1] Liou, T.-M., Hwang, J.-J., "Developing Heat Transfer and Friction in a Ribbed Rectangular Duct with Flow Separation at Inlet," *ASME Journal of Heat Transfer*, Vol. 114, August 1992, pp. 565-573.

[2] Han, J.C., Park, J.S., "Developing heat transfer in rectangular channels with rib turbulators," *Int. J. Heat Mass Transfer*, Vol. 31, No. 1, 1988, pp. 183-195.

[3] Rau, G., Çakan, M., Moeller, D., Arts, T., "The Effect of Periodic Ribs on the Local Aerodynamic and Heat Transfer Performance of a Straight Cooling Channel," *ASME Journal of Turbomachinery*, Vol. 120, April 1998, pp. 368-375.

[4] Sparrow, E.M., Tao, W.Q., "Enhanced Heat Transfer in a Flat Rectangular Duct with Streamwise-Periodic Disturbances at One Principal Wall," *ASME Journal of Heat Transfer*, Vol. 105, November 1983, pp. 851-861.

[5] Han, J.C., "Heat Transfer and Friction in Channels with Two Opposite Rib-Roughened Walls," *ASME Journal of Heat Transfer*, Vol. 106, November 1984, pp. 774-781.

[6] Taslim, M.E., Wadsworth, C.M., "An Experimental Investigation of the Rib Surface-Averaged Heat Transfer Coefficient in a Rib-Roughened Square Passage," *ASME Journal of Turbomachinery*," Vol. 119, April 1997, pp. 381-389.

[7] Liou, T.-M., Wu, Y.-Y., Chang, Y., "LDV Measurements of Periodic Fully Developed Main and Secondary Flows in a Channel with Rib-Disturbed Walls," *ASME Journal of Fluids Engineering*, Vol. 115, March 1993, pp. 109-114.

[8] Chanteloup, D., Juaneda, Y., Bölcs, A., "Combined 3D Flow and Heat Transfer Measurements in a 2-Pass Internal Coolant Passage of Gas Turbine Airfoils," Proceedings of the ASME Turbo Expo 2002, Amsterdam, The Netherlands.

[9] Casarsa, L., Arts, T., "Characterization of the Velocity and Heat Transfer Fields in an Internal Cooling Channel with High Blockage Ratio," Proceedings of the ASME Turbo Expo 2002, Amsterdam, The Netherlands.

[10] Moffat, R.J., "Describing the Uncertainties in Experimental Results," *Experimental Thermal and Fluid Science*, 1988, Vol. 1, pp. 3-17.

[11] Harder, K.J., Tiederman, W.G., "Influence of wall strain rate, polymer concentration and channel height upon drag reduction and turbulent structure," 1989, Technical Report PME-FM-89-1, Purdue University.